Human-Robot Visual Interface for 3D Steering of a Flexible, Bioinspired Needle for Neurosurgery

Eloise Matheson[1], Riccardo Secoli[1], Stefano Galvan[1] and Ferdinando Rodriguez y Baena [1]

Abstract— **Robotic minimally invasive surgery has been a subject of intense research and development over the last three decades, due to the clinical advantages it holds for patients and doctors alike. Particularly for drug delivery mechanisms, higher precision and the ability to follow complex trajectories in three dimensions (3D), has led to interest in flexible, steerable needles such as the programmable bevel-tip needle (PBN). Steering in 3D, however, holds practical challenges for surgeons, as interfaces are traditionally designed for straight line paths. This work presents a pilot study undertaken to evaluate a novel human-machine visual interface for the steering of a robotic PBN, where both qualitative evaluation of the interface and quantitative evaluation of the performance of the subjects in following a 3D path are measured. A series of needle insertions are performed in phantom tissue (gelatin) by the experiment subjects. User could adequately use the system with little training and low workload, and reach the target point at the end of the path with millimeter range accuracy.**

I. INTRODUCTION

Percutaneous intervention has attracted significant interest in Minimally Invasive Surgery (MIS) development, as it is performed through small ports through both the skin and soft tissue. To achieve complex paths in three-dimensional (3D) space, recent efforts have been applied to the development of tools which enable access to deep seated targets via curvilinear trajectories, such as flexible needles [1]. These needles can successfully reach targets whilst avoiding critical areas. The modeling and control of these needles have been an area of intense research, however comparatively few solutions exist for human-machine visual interfaces designed for intuitive steering along 3D paths.

Traditional interfaces for needle insertion tasks show pre-operative medical imaging during an operation. With MRI or CT based visual front ends, surgeons can see the 3D brain volumes, and navigate via views of the 2D slices of the Axial, Coronal and Sagittal planes of the anatomy. For 2D insertions of a tool, this is a proven interface, however for 3D insertions it can be difficult to correlate the slices to a 3D track [2]. Additionally, during surgery within highly compliant tissue, significant deformations can occur, which may alter the surgical scene. For instance, in neurosurgery, brain shift occurs as soon as the skull is opened due to a range of physiological, chemical, and physical factors, meaning pre-planned paths are no longer fully trusted by surgeons [3].

For real-time sensing of tools, preoperative images can be updated with co-registered intraoperative imaging, e.g. commonly from MRI or ultrasound sensors (US) [4]. However, the latency of generating MRI 3D volumes can be too high for real-time tracking of the needle [2], and such an embodiment would require an MRI-compatible needle system. US guidance is hence becoming the preferred option for various procedures [5]. US imaging, however, possesses a lower resolution than MRI and so, to help surgeons navigate 3D paths in the brain, a promising approach is to augment the imagery received intraoperatively in order to convey clearer visual information to the operator. This can be achieved with the use of augmented reality, or placing visual overlays on top of medical imagery [5], [6]. A visual interface for steering of magnetic micro-agents using US and other slow 2D imaging modalities was presented in [7], overlays tracking a target in 3D using US were presented in [8], and needle insertions for lung and liver insertions based on a 3D interface using CT was presented in [9]. However, these interfaces do not allow for intuitive navigation of insertions along a 3D path.

Inspiration for visual interfaces can come from other areas of 3D robotic steering. The main applications for human-machine interfaces towards 3D steering are applied to either Unmanned Aerial Vehicles (UAV) or Autonomous Underwater Vehicles (AUV), where a human operator maintains some control authority. There are many existing interfaces that share common characteristics. Such interfaces are designed to improve the situational awareness of the environment for the user [10], [11]. The interface needs to accurately represent reality, and often incorporates pre-mapped information as well as real-time imagery and updates. Augmented reality has often been shown to be an advantage for the user [12], though it is necessary to ensure the visual channel is not overloaded, confusing the operator. Similar design guidelines can be considered when developing a medical steering application.

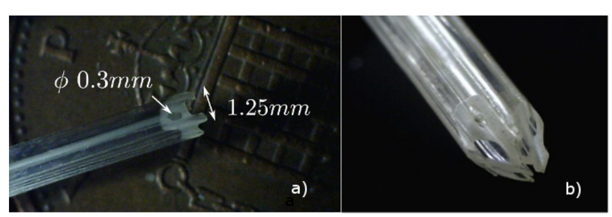

Fig. 1. **a)** Medical grade PBN needle segment cross-section; **b)** four part needle PBN assembled [taken from [13]
]

*This work has received funding from the European Unions EU Research and Innovation programme Horizon 2020 under grant agreement no 688279

[1]All authors are with the Mechatronics in Medicine Laboratory, Imperial College, London, United Kingdom f.rodriguez at imperial.ac.uk

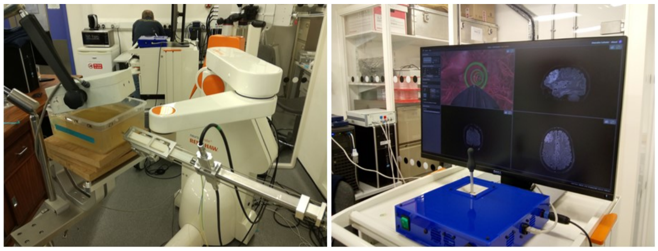

Fig. 2. Experimental setup showing the EM tracker, gelatin phantom and needle driver system (left), and human-machine visual interface and joystick (right).

This paper presents the integration of a novel human-machine visual interface for the intuitive navigation of a programmable bevel-tip needle (PBN) robotic system capable of steering along predefined 3D paths. The PBN, shown in Fig. 1, is a 4 segment, medical grade flexible needle that can steer in 3D [13], [14] by creating a relative offset between its bevel tipped segments that results in a bending moment as it is inserted into soft tissue. A human trial experiment (n=5) is carried out to evaluate the visual interface in terms of quantitative metrics (target reaching accuracy) and qualitative effort metrics (workload, intuition and preference ratings). The results from this pilot study will be used to improve the interface in preparation for a larger scale trial with surgeons.

II. Experimental Setup

The section briefly describes the robotic system experimental setup as shown in Fig. 2.

A. Mechatronic System

The PBN is actuated by a robotic system including an end-effector (EE) that holds the PBN, an actuation box, flexible transmission link, control box and a 2 degree-of-freedom (DOF) haptic joystick. Haptic feedback has not yet been incorporated for this study. The robotic system is integrated within a neurosurgical commercial robot suite, the neuromate® (Renishaw Plc), as shown in Fig. 3, by means of a bespoke connection to the last link of the robot arm and the EE.

B. Human-in-the-loop System Architecture

The software architecture is shown in Fig 5, using the Robotic Operating System (ROS, by the Open Source Robotics Foundation) as a framework, except in the case of communication between the robotic system and the visual interface, designed as a bespoke TCP connection with the commercial neuroinspire® front-end. The two axes of the joystick are directly mapped to the two main curvatures, which define the needle kinematics in the Parallel Transport Frame [14], [15]. The joystick mapping mocks airplane control stick behaviour, where a movement forward of the joystick achieves a curved path in the negative Z direction, as shown in Fig. 4, and a movement left of the joystick achieves a curved motion in the needle's positive Y axis.

Joystick commands are sent to an inverse model [17], coupled with a low level controller [14] that provides the

Fig. 3. Robotic system render: the robotic needle driver is integrated within the hardware of a neuromate® (Renishaw Plc)

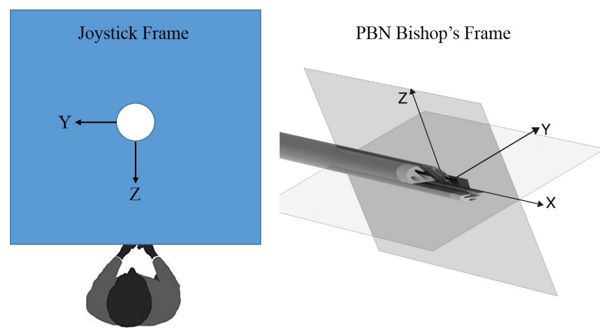

Fig. 4. Mapping of the joystick to needle curvature [adapted from [16]]

necessary offset configuration at the tip of the needle, to achieve the desired curvature. The cruise speed of insertion is fixed at 0.5 mm/s, and a foot-switch pedal allows the user to pause the motion. The 3D position of the needle is recorded at 40 Hz using electromagnetic (EM) sensors (Aurora, Northern Digital Inc. 5 DoF, RMS 0.9 mm, confidence interval 95% 1.8 mm) embedded within the tip of each segment. The signals from these sensors are fused in order to provide an estimate of the missing 6th DOF.

C. Visual Interface

The visual interface is a modified version of the commercial neurosurgical planning and intraoperative software neurosinspire™ (Renishaw plc). The standard release of the software provides three orthogonal views of the brain. The modified version includes a fourth window that visualizes the 3D navigation view. In this window, preoperative MRI images, segmented for the ventricles, vessels and/or tumour (target), and a preoperative CT scan, segmented for the skull, are used to build the obstacle map, which is used as the basis of the environment the surgeon must navigate through, shown in Fig. 6.

A path planner generates a feasible path [18] for the

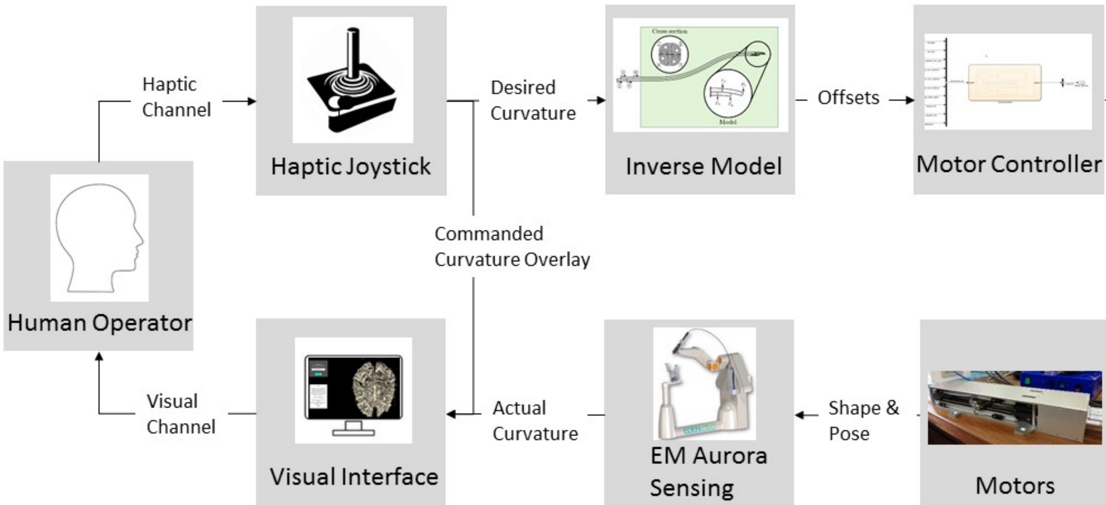

Fig. 5. System architecture

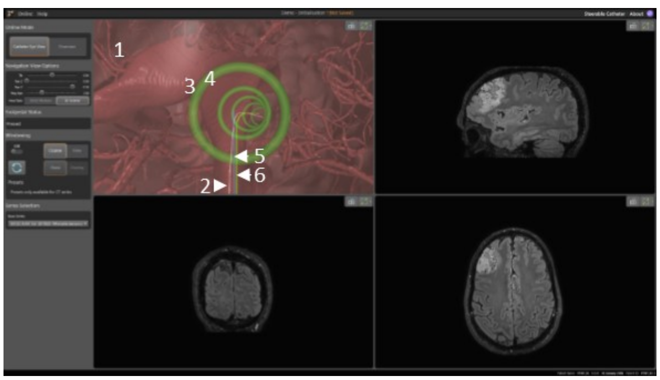

Fig. 6. Visual interface with Needle View Mode

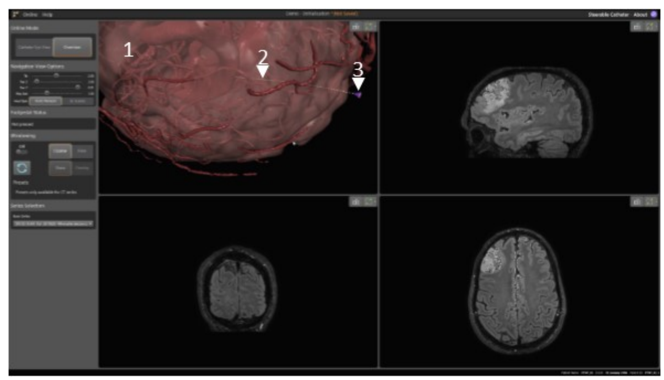

Fig. 7. Visual interface with Overview Mode

surgeon to follow, from the entry point of the skull to the target pose, that avoids all obstacles within a safe radius. If the surgeon strays off this path by a predefined magnitude, then the system will re-plan a new path [16] to the target if one exists. If no such path exists, then the last generated path is always displayed to the surgeon, see Fig 8. The path that the surgeon should follow, as well as the current configuration of the tip of the needle, can be visually depicted to the surgeon in multiple ways. In this design, the navigation window shows a 2D render of a 3D environment, where the surgeon has a first person viewpoint when navigating the needle (called 'Needle View Mode', see Fig 6), though they can also choose to stop steering and look from a third person view (called 'Overview Mode', see Fig 7). This design was chosen based on feedback from an advisory group of neurosurgeons, as it was hypothesized that it would be more intuitive for a surgeon to navigate in first person view, though the third person overview was also desired in order to show a similar viewpoint as normally seen when looking at standard MRI volumes. Each of the four individual windows can be maximized as needed. The navigation window in Needle View Mode (Fig 6) has the following visual components;

1) Segmented anatomy as obstacle map
2) Optimal path depicted as a white line
3) Waypoints represented as rings, where the centre of the ring lies on the optimal path
4) Colour of the rings representing the error of the needle tip pose to the path
5) Blue ray representing the 'Actual Overlay'
6) Green ray representing the 'Commanded Overlay'

The navigation window in Overview Mode (Fig 7) has the following visual components;

1) Segmented anatomy as obstacle map
2) Optimal path depicted as a dashed white line
3) Current pose of the needle tip shown as a purple cone

The 'Actual Overlay' represents the predicted path the needle will follow based on the current configuration of the motors, and the forward kinematic model of the needle. The

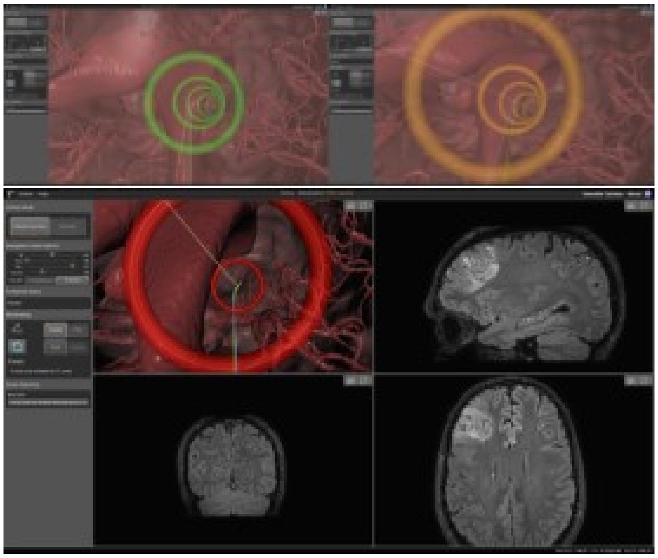

Fig. 8. Needle view mode when error is low (top left), getting higher (top right) and high, hence triggers path re-planning (bottom)

'Commanded Overlay' represents the path the needle should follow based on the configuration of the joystick. The colour of the ring represents a metric for the error indicating how far the needle is from the path, and fuses the magnitude of position and orientation error into a value between 0 (directly on the path) and 1 (far from the path, in which case a path re-planning event is triggered).

III. Experiment Design

To validate the real-time performance of the visual interface and tele-operated joystick for the PBN navigation system, a human studies trial measured the performance of multiple users under controlled conditions. As this trial collects personal data, ethical approval was sought and approved by Imperial College Londons Joint Research Compliance Office, with ICREC reference 18IC4564.

Two experimental protocols were designed as in Table I. The task was to steer a needle through a phantom brain tissue (bovine gelatin of 250 bloom, 6 wt%, clear-transparent color), while navigating a curvilinear path in 3D. Protocol A allowed the subject to familiarize and train with the system via 2 training insertions, and also to gather qualitative feedback from their initial understanding of the interface. They were asked to answer a user survey of 6 questions regarding Layout, Understanding and Visual Cues directly, after finishing 2 insertion tasks. User surveys consisted of questions asked using the Likert Scale[19] from 1 to 5, where 1 represented 'Strongly Disagree', and 5 'Strongly Agree'. No quantitative data were collected during these insertions.

Protocol B took place directly after Protocol A, and measured the performance of the user in reaching a target (for a total of 5 insertions each, all with the same path) as well as evaluating workload and subjective evaluation of the visual interface. To evaluate workload, the NASA-TLX chart [20] was used to measure six single-level 20 point sub-scaled questions around: mental, physical, and temporal task demands, perceived performance, effort and frustration. To evaluate the visual interface, users were asked to complete a user survey of 15 questions in three areas - Navigation, Skill Level and Visualization - and answer open ended questions about what the positive and negative aspects of the interface were.

TABLE I
EXPERIMENT PROTOCOL DESCRIPTIONS

Prot.	Instructions	Metric
A	-You will undertake two needle insertions - The foot pedal enables movement - The 3D navigation window can be maximized or minimized at will - You can change to overview mode, but you must release the foot pedal - You cannot ask further questions about the meaning of the visual interface or task	- User Survey
B	- The meanings of the cues as in Section II-C - You can ask any questions if aspects of the visual interface are not clear -You will undertake five needle insertions - Stop navigating when you think you have reached the end of the path - Time to complete the task is not evaluated	- User Survey - NASA TLX - Target reaching error

IV. Results and Discussion

A total of five male subjects, all between the ages of 20 - 30, who were not color blind and had healthy hand ability, participated in the study.

A. Protocol A

The user survey answers for Protocol A after their training insertions are described in Fig 9. Notably, all subjects were neutral or (strongly) agreed that the visualization meaning and colour coding were easy to interpret and logical, however 40% subjects disagreed that it was easy to understand the system without further instructions, and 20% subjects found the different colours in the visual system to be hard to distinguish. Future iterations of the visual design will seek to make the colours more distinguishable, and to ensure that the user understands the meaning of the visual elements before operating the system either via training or a written description.

B. Protocol B

The collated results of the user survey are shown in Fig 9. All questions had an average of a positive result. The open ended responses highlighted that there were sometimes unexpected changes in the path (transition between ring colours very fast and distracting) when path re-planning was triggered or due to noise in the needle pose estimation. They also commented that it was difficult to correlate the axis in the Overview Mode to those in the Catheter View Mode, and that the blue overlay was not of much use. However, subjects commented that the joystick was very intuitive to use, the colour coding of the path and rings was particularly useful

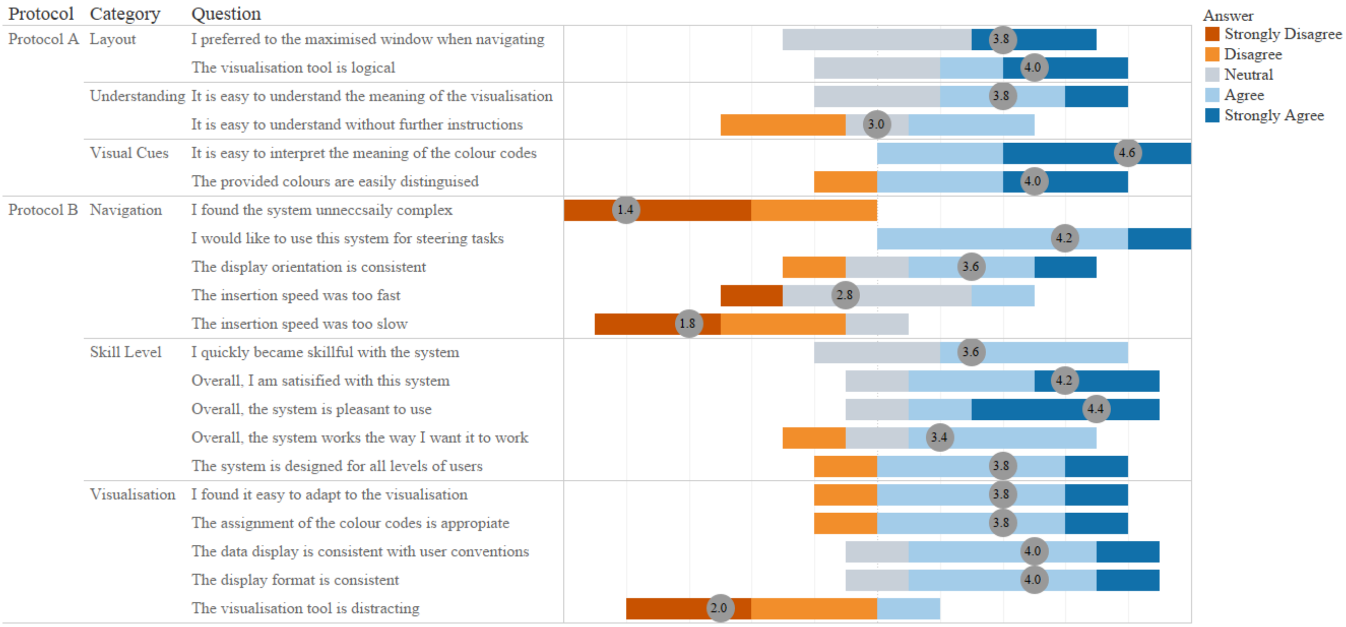

Fig. 9. Likert Scale chart showing the subject responses. The average score is shown in the grey circle, and the collated answers are shown by colours, where the percent of subject answers in the scale is shown by the size of the boxes.

for navigation and that the visual interface was intuitive and immersive. The results of the NASA TLX chart can be seen in Fig 10, indicating the interface was easy to use and that the task was not demanding. It will be interesting in future studies to increase the task difficulty.

To evaluate the quantitative performance of the system, the final pose of the needle was compared to that of the final pose of the path i.e. the target. The position error was the Euclidean distance between the needle and target positions. The orientation error was calculated as the screw angle between the needle approach angle and the orientation of the target. Fig. 11 shows the mean and standard deviation of the magnitude of position and orientation error for the final position reached by each subject over their 5 trials. The final error of the system over all subjects ($n = 5$ for a total of 25 insertions) was 4.3 ± 1.5 mm and 12.9 ± 7.0 degrees. Normal distribution of the position error was found (assessed by Shapiro-Wilk Normality test, $p > 0.9$) however normal distribution of the orientation errors (assessed by Shapiro-Wilk Normality test, $p < 0.001$) was not confirmed. The path following error metric was not used in this assessment, as the path re-planner was triggered when the needle moved off the path, creating new, feasible path.

The goal was to reach the end of the path - users were not specifically instructed that they should aim for the best precision in both position and orientation. The results in Fig. 11 (see Subjects 1 and 5 in particular) show that subjects with low orientation errors and spread had higher positional error and larger spread, indicating these subjects considered one metric with higher priority. It is expected that future trials with a better description of the task, as well as system indications on desired position and orientation/rotation, would result in lower rotational errors.

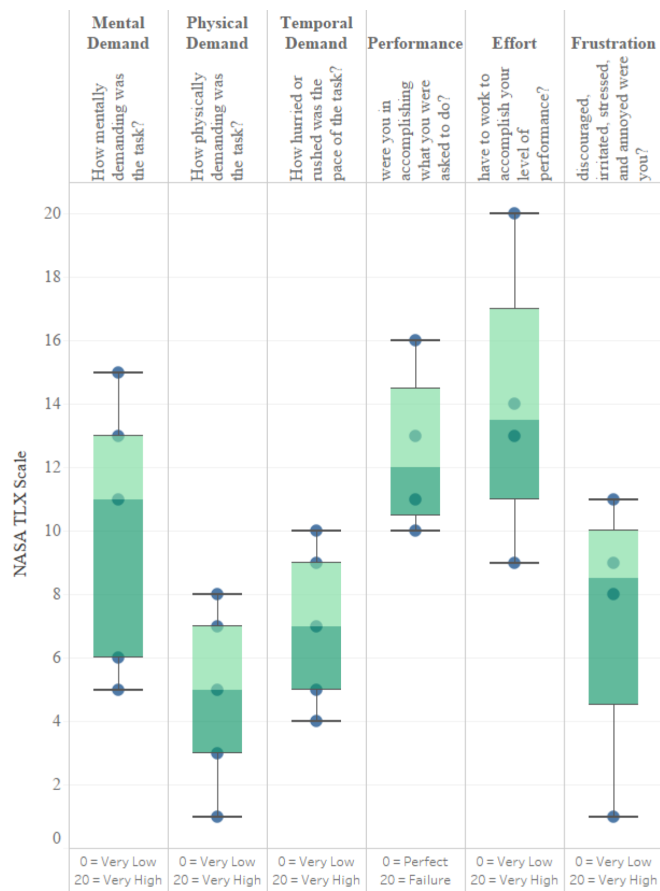

Fig. 10. NASA TLX Scale results to measure the workload.

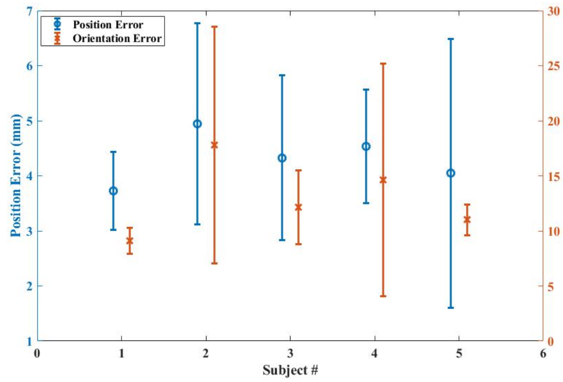

Fig. 11. Mean error in target reaching for each subject where the error bars represent standard deviation

Considering these pilot study results, based on the observed standard deviations and expecting a practically relevant mean difference of 25% for the target reaching metric of position accuracy, a recommended sample size for a future study would be n = 30 (for statistical power 1 - $\beta = 0.8$ and significance level of $\alpha = 0.05$).

Notably, the subject could control the system past the final path reference point, as no information was provided about task completion. Taking the final error measurements from the last point of the reference path to the closest point on the needle trajectory, ignoring any overshoot by the subject, the final error reduces to 3.2 ± 0.4 mm and 11.7 ± 2.3 degrees. This performance can be achieved if system notifications on task completion are provided. These results are clinically relevant, as literature suggests that neurosurgical needle insertions with accuracy of 3.2 ± 1.4 mm are common when using stereotactic frames [21].

V. CONCLUSION

This study describes the integration of a novel human-machine visual interface designed for the intuitive navigation of Programmable Bevel-tip Needles during neurosurgery procedures. A pilot study was run to provide initial qualitative and quantitative evaluation of the interface. This will be used to inform a larger scale evaluation of the visual interface by surgeons, where haptic feedback and shared control strategies will also be incorporated in order to find the best combination of human-machine interface modalities.

ACKNOWLEDGMENT

Integration of the visual interface within the neurosinpire^{TM} framework was helped by RENISHAW plc, a member of the EDEN2020 consortium (www.eden2020.eu).

REFERENCES

[1] J. A. Engh, G. Podnar, D. Kondziolka, and C. N. Riviere, "Toward effective needle steering in brain tissue," in *2006 International Conference of the IEEE Engineering in Medicine and Biology Society*, Aug 2006, pp. 559–562.

[2] M. Ries, B. D. de Senneville, S. Roujol, Y. Berber, B. Quesson, and C. Moonen, "Real-time 3d target tracking in mri guided focused ultrasound ablations in moving tissues," *Magnetic Resonance in Medicine*, vol. 64, no. 6, pp. 1704–1712, 2010. [Online]. Available: http://dx.doi.org/10.1002/mrm.22548

[3] I. J. Gerard, M. Kersten-Oertel, K. Petrecca, D. Sirhan, J. A. Hall, and D. L. Collins, "Brain shift in neuronavigation of brain tumors: A review," *Medical Image Analysis*, vol. 35, pp. 403 – 420, 2017.

[4] D. H. Iversen, W. Wein, F. Lindseth, G. Unsgrd, and I. Reinertsen, "Automatic intraoperative correction of brain shift for accurate neuronavigation," *World Neurosurgery*, vol. 120, pp. e1071 – e1078, 2018.

[5] H. J. Scholten, A. Pourtaherian, N. Mihajlovic, H. H. M. Korsten, and R. A Bouwman, "Improving needle tip identification during ultrasound-guided procedures in anaesthetic practice," *Anaesthesia*, vol. 72, no. 7, pp. 889–904, Jul 2017.

[6] S. R. Clendenen, S. A. Candler, M. D. Osborne, S. C. Palmer, S. Duench, L. Glynn, and S. M. Ghazi, "Needle placement for piriformis injection using 3-D imaging," *Pain Physician*, vol. 16, no. 3, pp. E301–310, 2013.

[7] M. Kaya, A. Denasi, S. Scheggi, E. Abahca, C. Yoon, D. H. Gracias, and S. Misra, "A multi-rate state observer for visual tracking of magnetic micro-agents using 2d slow medical imaging modalities," 10 2018, pp. 1–8.

[8] J. Chevrie, N. Shahriari, M. Babel, A. Krupa, and S. Misra, "Flexible needle steering in moving biological tissue with motion compensation using ultrasound and force feedback," *IEEE Robotics and Automation Letters*, vol. 3, no. 3, pp. 2338–2345, July 2018.

[9] P. Bhattacharji and W. Moore, "Application of Real-Time 3D Navigation System in CT-Guided Percutaneous Interventional Procedures: A Feasibility Study," *Radiology Research and Practice*, vol. 2017, p. 7, 2017. [Online]. Available: 10.1155/2017/3151694

[10] M. Mulder, J. Mulder, and H. G. Stassen, "Cybernetics of tunnel-in-the-sky displays. ii. curved trajectories," vol. 5, 10 1999.

[11] C. Yuan, F. Recktenwald, and H. A. Mallot, "Visual steering of uav in unknown environments," in *2009 IEEE/RSJ International Conference on Intelligent Robots and Systems*, Oct 2009, pp. 3906–3911.

[12] G. L.Calhoun, M. H.Draper, M. F. Abernathy, M. Patzek, and F. Delgado, "Synthetic vision system for improving unmanned aerial vehicle operator situation awareness," in *Proc. SPIE 2005*, vol. 5802, 2005, pp. 5802 – 5802 – 12. [Online]. Available: https://doi.org/10.1117/12.603421

[13] T. Watts, R. Secoli, and F. Rodriguez y Baena, "A mechanics-based model for 3-d steering of programmable bevel-tip needles," *IEEE Transactions on Robotics*, vol. PP, pp. 1–16, 12 2018.

[14] R. Secoli, F. Rodriguez, and Baena, "Experimental validation of curvature tracking with a programmable bevel-tip steerable needle," in *2018 International Symposium on Medical Robotics (ISMR)*, March 2018, pp. 1–6.

[15] R. Secoli and F. R. y Baena, "Adaptive path-following control for bio-inspired steerable needles," in *2016 6th IEEE International Conference on Biomedical Robotics and Biomechatronics (BioRob)*, June 2016, pp. 87–93.

[16] F. Liu, A. Garriga-Casanovas, R. Secoli, and F. Rodriguez y Baena, "Fast and adaptive fractal tree based path planning for programmable bevel tip steerable needles," *IEEE Robotics and Automation Letters*, vol. 1, pp. 1–1, 07 2016.

[17] T. Watts, R. Secoli, and F. Rodriguez y Baena, "Needle steerability measures: Definition and application for optimized steering of the programmable bevel-tip needle," in *15th IEEE International Conference on Robotics and Biomimetics ROBIO, Malaysia, December 2018*, in press.

[18] M. Pinzi, S. Galvan, and F. Rodriguez y Baena, "The adaptive hermite fractal tree (ahft): a novel surgical 3d path planning approach with curvature and heading constraints," *International Journal of Computer Assisted Radiology and Surgery*, Feb 2019.

[19] J. Robinson, *Likert Scale*. Dordrecht: Springer Netherlands, 2014, pp. 3620–3621.

[20] S. G. Hart and L. E. Stavenland, "Development of nasa-tlx (task load index): Results of empirical and theoretical research," pp. 139–183, 1988.

[21] P.-F. D'Haese, S. Pallavaram, P. E. Konrad, J. Neimat, J. M. Fitzpatrick, and B. M. Dawant, "Clinical accuracy of a customized stereotactic platform for deep brain stimulation after accounting for brain shift," *Stereotactic and Functional Neurosurgery*, no. 2, pp. 81–87, 2010.